Exploiting the mutanome for tumor vaccination

John C. Castle[1,5], Sebastian Kreiter[1,5], Jan Diekmann[1], Martin Löwer[1], Niels van de Roemer[1,2], Jos de Graaf[1], Abderraouf Selmi[1,] Mustafa Diken[1], Sebastian Boegel[1,2], Claudia Paret[1], Michael Koslowski[1], Andreas N. Kuhn[1,3], Cedrik M. Britten[2,3], Christoph Huber[1,3], Özlem Türeci[4,6] and Ugur Sahin[1,2,3,6]

[1]TRON - Translational Oncology at the University Medical Center Mainz, 55131 Mainz, Germany
[2]University Medical Center of the Johannes Gutenberg-University Mainz, III. Medical Department, Mainz, Germany
[3]Ribological, Biontech AG, Mainz, 55131, Germany
[4]Ganymed Pharmaceuticals AG, Mainz, Germany
[5]These authors contributed equally to the first authorship
[6]These authors contributed equally to the last authorship

Running title: B16 melanoma T-cell druggable mutanome

Keywords: tumor immunity, cancer immunotherapy, personalized medicine, tumor mutations

Financial support: This work was supported by the by the program for innovative molecular and cellular therapies of the Federal Ministry of Education and Research (BMBF).

Conflict of interest: U. Sahin, C. Huber, C. Britten and A. Kuhn are associated with BioNTech AG (Mainz, Germany), a company, which develops RNA-based cancer vaccines. U. Sahin, S. Kreiter, Ö. Türeci, A. Selmi, J. Castle, J. Diekmann, C. Britten and M. Diken are inventors on patent applications, in which parts of this paper are covered.

Corresponding author: Ugur Sahin (sahin@uni-mainz.de).
Address: Langenbeckstr 1,55131, Mainz, Germany
Phone: +49 6131 178054
Fax: +49 6131 178055

Abstract

Multiple genetic events and subsequent clonal evolution drive carcinogenesis, making disease elimination with single targeted drugs difficult. The multiplicity of gene mutations derived from clonal heterogeneity therefore represents an ideal setting for multi-epitope tumor vaccination. Here we used NGS exome resequencing to identify 941 non-synonymous somatic point mutations in B16F10 murine melanoma cells, with 589 of those mutations in expressed genes. Potential driver mutations occurred in classical tumor suppressor genes and genes involved in proto-oncogenic signaling pathways that control cell proliferation, adhesion, migration and apoptosis. *Aim1* and *Trrap* mutations known to be altered in human melanoma were included among those found. The immunogenicity and specificity of 50 validated mutations was determined by immunizing mice with long peptides encoding the mutated epitopes. One-third of these peptides were found to be immunogenic, with 60% in this group eliciting immune responses directed preferentially against the mutated sequence as compared to the wild type sequence. In tumor transplant models, peptide immunization conferred in vivo tumor control in protective and therapeutic settings, thereby qualifying mutated epitopes that include single amino acid substitutions as effective vaccines. Together, our findings provide a comprehensive picture of the mutanome of B16F10 melanoma which is used widely in immunotherapy studies. Additionally, they offer insight into the extent of the immunogenicity of non-synonymous base substitution mutations. Lastly, they argue that the use of deep sequencing to systematically analyze immunogenicity mutations may pave the way for individualized immunotherapy of cancer patients.

Introduction

The advent of next generation sequencing (NGS) technology has added a new dimension to genome research by generating ultra-fast and high-throughput sequencing data in an unprecedented manner (1). The first mouse tumor genome has been published (2) and the genomes and exomes (the RNA-encoding genomic sequence) of several human primary tumors and cell lines have been dissected (3-5). As cancerogenesis is driven by mutations, the capability of NGS to provide a comprehensive map of somatic mutations in individual tumors (the "mutanome") provides a powerful tool to better understand and intervene against cancer.

The first views into the human mutanome revealed by NGS show that human cancers carry 10s to 100s of non-synonymous mutations. Mutations shared among patients suffering from one tumor entity allow targeted approaches, as exemplified by small-molecule inhibitors targeting the bcr-abl translocation present in 90% of CML patients. However, shared mutations are rare and the great majority of mutations are patient specific, which has hindered exploitation of the mutanome for the development of broadly applicable drugs.

Once mutations have been identified, major efforts are typically invested to determine the mutation functional impact, such as cancer driver versus passenger status, to form a basis for selecting suitable therapeutic targets. However, little attention has been devoted to either define the immunogenicity of these mutations or characterize the immune responses they elicit. From the immunological perspective, mutations may be particularly potent vaccination targets as they can create neo-antigens that are not subject to central immune tolerance. Whereas for other tumor antigen categories there is the likelihood of downregulation in metastases, mutations that

occur in early tumor development are sustained in advanced disease (5). Indeed, several immunogenic cancer mutations have been described in mice and patients. Some mutations are capable of inducing rejection of tumors in mice (6, 7) and others are targets of spontaneously occurring dominant immune responses in patients with malignant melanoma (8). However, it is not known whether these examples represent rare cases of incidental immunogenicity or the tip of the iceberg of potentially useful vaccine targets.

We addressed this question in a systematic approach by embarking on a study to determine the proportion of non-synonymous mutations that are able to induce a target specific immune response in the syngeneic host. The aim is to define and validate molecular alterations in the B16F10 melanoma model, the most widely used model for experimental cancer therapies, and determine their immunogenicity in C57BL/6 mice. In doing so, we completed the first mouse tumor exome and identified 962 non-synonymous somatic point mutations of high confidence, of which 563 occur in expressed genes. We demonstrate for the first time a correlation between tumor mutations and the epitope landscape by *in vivo* data, showing that many non-synonymous somatic mutations in tumors are immunogenic and confer antitumoral vaccine activity.

Methods

Samples

C57BL/6 mice (Jackson Laboratories) were kept in accordance with federal and state policies on animal research at the University of Mainz. B16F10 melanoma cell line was purchased in 2010 from the American Type Culture Collection (Product: ATCC CRL-6475, Lot Number: 58078645). Early (3^{rd}, 4^{th}) passages of cells were used for tumor experiments. Re-authentification of cells has not been performed since receipt.

Next-generation sequencing

DNA and RNA from B16F10 cells and DNA from C57BL/6 tail tissue were extracted in triplicate. Exome capture for DNA resequencing was performed in triplicate using the Agilent mouse whole-exome Sure-Select assay (9). Using 5 μg of total RNA, barcoded mRNA-seq cDNA libraries were prepared in triplicate using a modified Illumina mRNA-seq protocol. All libraries were sequenced on an Illumina HiSeq2000 to generate 50 nt reads. Sequence reads from were preprocessed according to the Illumina standard protocol. RNA reads were aligned to the mm9 reference genome (10) and transcriptome using bowtie (11), and gene expression was determined by comparison to RefSeq transcript coordinates, followed by normalization to RPKM units (Reads which map per Kilobase of transcript per Million mapped reads) (12). DNA reads were aligned to the reference genome using bwa (13). Mutations were identified using three algorithms and assigned a false discovery rate (FDR) confidence value (Löwer *et al*., submitted). Detailed methods are described in supplemental information.

Mutation selection, validation and function

Mutations were selected that were: (i) present in all B16F10 and absent in all C57BL/6 triplicates, (ii) FDR ≤0.05, (iii) homogeneous in C57BL/6, (iv) occur in a RefSeq transcript, and (v) cause non-synonymous changes. Further mutation selection criteria were occurence in B16F10 expressed genes (median RPKM across replicates >10) and in an MHC-binding peptide based on the Immune Epitope Database (IEDB) (14). For validation, variants were amplified from DNA from B16F10 cells and C57BL/6 tail tissue, subjected to Sanger sequencing, and results visually examined (Supplemental Information). DNA-derived mutations were classified as validated if confirmed by either Sanger sequencing or the B16F10 RNA-Seq reads. Algorithms SIFT (15) and POLYPHEN-2 (16) were used to predict mutation functional impact. They predict the functional significance of an amino acid on protein function using the location of protein domains and cross-species sequence conservation. Ingenuity IPA was used to infer gene function.

Synthetic peptides and adjuvants

All peptides including vesiculo-stomatitis virus nucleoprotein (VSV-NP_{52-59}) and tyrosinase-related protein 2 ($Trp2_{180-188}$) were purchased from Jerini Peptide Technologies (Berlin, Germany). Synthetic peptides were 27 amino acids long with the mutated (MUT) or wild type (WT) amino acid on position 14. Polyinosinic:polycytidylic acid (poly(I:C), InvivoGen) was used as subcutaneously injected adjuvant.

Immunization of mice

Age-matched female mice C57BL/6 mice were injected subcutaneously with 100 µg peptide and 50 µg poly(I:C) formulated in PBS (200 µl total volume) into the lateral flank (5 mice per group). Every group was immunized on day 0 and day 7 with two different mutation coding peptides, one peptide per flank. Mice were sacrificed 12 days after the initial injection and splenocytes isolated for immunological testing.

Enzyme-linked immunospot assay

Enzyme-linked immunospot (ELISPOT) assay (17) and generation of syngeneic bone marrow derived dendritic cells (BMDCs) as stimulators were previously described (18). BMDCs were either peptide pulsed (2 µg/ml), or transfected with *in vitro* transcribed (IVT) RNA coding for the indicated mutation or for control RNA (eGFP-RNA). Sequences representing two mutations, each comprising 50 amino acids with the mutation on position 25 and separated by a glycin/serine linker of 9aa were cloned into the pST1-2BgUTR-A120 backbone (19). *In vitro* transcription from this template and purification were previously described (20). For the assay, 5×10^4 peptide or RNA engineered BMDCs were coincubated with 5×10^5 freshly isolated splenocytes in a microtiter plate coated with anti-IFN-γ antibody (10 µg/mL, clone AN18; Mabtech). After 18 hours at 37°C, cytokine secretion was detected with an anti-IFN-γ antibody (clone R4-6A2; Mabtech).

B16 melanoma tumor model

For tumor vaccination, 7.5×10^4 B16F10 melanoma cells were inoculated s.c. into the flanks of C57BL/6 mice. Prophylactic immunization with mutation-specific peptide was performed 4 days

before and on days 2 and 9 after tumor inoculation. Therapeutic immunization with the peptide vaccine was administered on days 3 and 10 after tumor injection. The tumor sizes were measured every three days and mice were sacrificed when tumor diameter reached 15 mm.

Results

Identification of non-synonymous mutations in B16F10 mouse melanoma

Our objective was to identify potentially immunogenic somatic point mutations in B16F10 mouse melanoma by NGS and to test these for *in vivo* immunogenicity by peptide vaccination of mice measuring elicited T-cell responses by ELISPOT assay (Figure 1A). We sequenced the exomes of the C57BL/6 wild type background genome and of B16F10 cells, each with triplicate extractions and captures. For each sample, more than 100 million single-end 50 nt reads were generated (Table S1). Of these 80%, align uniquely to the mouse mm9 genome and 49% align on target, demonstrating successful target enrichment and resulting in over 20-fold coverage for 70% of the target nucleotides in each individual sample of the triplicates. RNA-Seq of B16F10 cells, also profiled in triplicate, generated a median of 30 million single-end 50 nt reads for each sample, of which 80% align to the mouse transcriptome.

DNA reads (exome-capture) from B16F10 and C57BL/6 were analyzed to identify somatic mutations. Copy number variation analysis (21) demonstrated DNA amplifications and deletions in B16F10, including the homozygous deletion of tumor suppressor *Cdkn2a* (Cyclin-dependent kinase inhibitor 2A, p16Ink4A). To identify possibly immunogenic mutations, we identified 3570 somatic point mutations at FDR ≤ 0.05 (Figure 1B). The most frequent class of mutations was C>T/G>A transitions, as often results from ultraviolet light (22). Of these somatic mutations, 1392 occur in transcripts, with 126 mutations in untranslated regions. Of the 1266 mutations in coding regions, 962 cause non-synonymous protein changes and of these 563 occur in expressed genes (Figure 1B, Table S2).

Assignment of identified mutations to carrier genes and validation

Table S2 lists the 962 genes containing non-synonymous somatic point mutations, subcellular localization and gene type. Noteworthy, many of the mutated genes have been previously associated with cancer phenotypes. Mutations were found in established tumor suppressor genes, including *Pten*, *Trp53 (*also called *p53)*, and *Tp63*. In *Trp53,* the best established tumor suppressor (23), the asparagine to aspartic acid mutation at protein position 127 (p.N127D) is localized in the DNA binding domain and predicted to alter function. *Pten* contained two mutations (p.A39V, p.T131P), both of which are predicted to have deleterious impact on protein function. The p.T131P mutation is adjacent to a mutation (p.R130M) shown to diminish phosphatase activity (24).

Several mutations occur in genes associated with DNA repair pathways, such as *Brca2* (breast cancer 2, early onset), *Atm* (ataxia telangiectasia mutated), *Ddb1* (damage-specific DNA binding protein 1) and *Rad9b* (RAD9 homolog B). Furthermore, we found mutations in other tumor associated genes, including *Aim1* (tumor suppressor "Absent In Melanoma 1"), *Flt1* (oncogene *Vegr1*, fms-related tyrosine kinase 1), *Pml* (tumor suppressor "promyelocytic leukemia"), *Fat1* ("FAT tumor suppressor homolog 1"), *Mdm1* (TP53 binding nuclear protein), *Mta3* (metastasis associated 1 family, member 3), and *Alk* (anaplastic lymphoma receptor tyrosine kinase). A mutation occurs at p.S144F in *Pdgfra* (platelet-derived growth factor receptor, alpha polypeptide), a cell-membrane-bound receptor tyrosine kinase of the MAPK/ERK pathway, previously identified in tumors (25). *Casp9* (caspase 9, apoptosis-related cysteine peptidase) proteolytically cleaves poly(ADP-ribose) polymerase (PARP), regulates apoptosis, and has been

linked to several cancers (26); here, we found a mutation at p.L222V that may impact PARP and apoptosis signaling.

Interestingly, no mutations were found in *Braf*, *c-Kit*, *Kras* or *Nras*. However, mutations were identified in *Rassf7* (RAS-associated protein) (p.S90R), *Ksr1* (kinase suppressor of ras 1) (p.L301V), and *Atm* (PI3K pathway) (p.K91T), all of which are predicted to have significant impact on protein function. *Trrap* (transformation/transcription domain-associated protein) was identified earlier this year in human melanoma specimens as a novel potential melanoma target (27). In B16F10, a *Trrap* mutation occurs at p.K2783R which is predicted to disturb the overlapping phosphatidylinositol kinase (PIK)-related kinase FAT domain.

From the 962 identified non-synonymous mutations, we selected 50 mutations for PCR-based validation and immunogenicity testing. Selection criteria included low FDR, location in an expressed gene and predicted immunogenicity (Methods). Noteworthy, all 50 mutations validated (Table 1, Figure 1B) and can be visualized in Figure 1C.

In vivo testing of immunogenicity testing with mutation-representing long peptides

We employed long peptides as antigens for immunogenicity testing of these mutations. Long peptides have many advantages as induction of antigen-specific $CD8^+$ as well as $CD4^+$ T-cells and processing to be presented on MHC molecules (28). Uptake is most efficiently done by dendritic cells, which are optimal for priming a potent T-cell response. Fitting peptides, in contrast, do not require trimming and are loaded exogenously on all cells expressing MHC

molecules, including non-activated B and T-cells, leading to induction of tolerance and fratricide.

For each of the 50 validated mutations, we designed peptides of 27 amino acids length with the mutated or wild type amino acid positioned centrally. Thus, all potential MHC class I and class II epitope of 8 to 14 amino acid length carrying the mutation could be processed from this precursor peptide. As adjuvant for peptide vaccination we used poly(I:C) which promotes cross presentation and increase vaccine efficacy (29).

The 50 mutations were tested *in vivo* in mice for induction of T-cells. Impressively, 16 out of 50 mutation-coding peptides were found to elicit immune responses in immunized mice. The induced T-cells displayed different reactivity patterns (Table 2). Eleven peptides induced an immune response preferentially recognizing the mutated epitope, including mutations 30 (MUT30, *Kif18b*) and 36 (MUT36, *Tm9sf3*) (Figure 2A). ELISPOT testing revealed strong mutation-specific immune responses without cross reactivity against the wild-type peptide or an unrelated control peptide (VSV-NP). With five peptides, including mutations 05 (MUT05, *Eef2*) and 25 (MUT25, *Plod2*) (Figure 2A), immune responses with comparable recognition of both the mutated as well as the wild-type peptide were obtained. The majority of mutated peptides were not capable of inducing significant T-cell responses, as shown by mutations 01 (MUT01, *Fzd7*), 02 (MUT02, *Xpot*), and 07 (MUT07, *Trp53*). Immune responses induced by several of the discovered mutations were in the range of the immunogenicity (500 spots/5x10^5 cells) generated by immunizing mice with the positive control MHC-class I epitope from the murine melanoma tumor antigen tyrosinase-related protein 2 ($Trp2_{180-188}$, Figure 2A) (30, 31).

For peptides that induce a strong mutation-specific T-cell response, we confirmed immune recognition by an independent approach. Instead of long peptides, *in vitro* transcribed RNAs (IVT RNA) coding for the mutated peptide fragments MUT17, MUT30 and MUT44 were used for the immunological read-out. BMDCs transfected with mutation-coding RNA or irrelevant RNA served as antigen presenting cells (APCs) in an ELISPOT assay, whereas spleen cells of immunized mice served as effector cell population. BMDCs transfected with MUT17, MUT30 and MUT44 encoding mRNA were specifically and strongly recognized by splenocytes of mice immunized with the respective long peptides (Figure 2B). Significantly lower reactivity against control RNA-transfected BMDCs was recorded, which is likely due to the unspecific activation of the BMDCs by the single stranded RNA (student´s t-test; MUT17: $p = 0.0024$, MUT30: $p = 0.0122$, MUT44: $p = 0.0075$). These data confirm that the induced mutation-specific T-cells in effect recognize endogenously processed epitopes.

Two mutations that induce a preferred recognition of mutated epitopes are in genes *Actn4* and *Kif18b*. The somatic mutation in ACTN4 (actinin, alpha 4) is at p.F835V in the calcium binding "EF-hand" protein domain. While both SIFT and POLYPHEN predict a significant impact of this mutation on protein function, the gene is not an established oncogene. However, mutation-specific T-cells against ACTN4 have been recently associated with a positive patient outcome (32). KIF18B (kinesin family member 18B) is a kinesin with microtubule motor activity and ATP and nucleotide binding that is involved in regulation of cell division (33) (Figure 3). The DNA sequence at the position encoding p.K739 is homogeneous in the reference C57BL/6, whereas B16F10 DNA reads reveal a heterozygous somatic mutation. Both nucleotides were detected in the B16F10 RNA-Seq reads and validated by Sanger sequencing. KIF18B has not been previously associated with a cancer phenotype. The mutation p.K739N is not localized in a

known functional or conserved protein domain (Figure 3, bottom) and thus most likely is a passenger rather than a driver mutation. These examples suggest a lack of correlation between the capability of inducing mutation-recognizing immune response and a functional relevance.

In vivo assessment of antitumoral activity of vaccine candidates

We assessed whether immune responses elicited *in vivo* translate in antitumoral effects in tumor bearing mice using mutations MUT30 (mutation in Kif18b) and MUT44 as examples. Both mutations induce a strong immune reaction preferentially against the mutated peptide and are endogenously processed (Figure 2A, B). The therapeutical potential of vaccinating with mutated peptides was explored by immunizing mice with MUT30, MUT44 or Trp2 and adjuvant 3 and 10 days after grafting with $7.5x10^5$ B16F10. Growth of tumors was inhibited by both mutation encoding peptides as compared to the control groups (Figure 4A). Remarkably, vaccinating with MUT30 and MUT44 peptides induced tumor growth inhibition equal to the established Trp2 peptide. Furthermore, as B16F10 is a very aggressive tumor, we also tested protective immune responses. Mice were immunized with MUT30 peptide, inoculated s.c. with $7.5x10^5$ B16F10 cells 4 days later and boosted with MUT30 immunization 2 and 9 days after tumor challenge. Complete tumor protection and survival of 40% of the mice treated with MUT30 were observed, whereas all mice in the control treated group died within 44 days (Figure 4B left). In the mice that developed tumors despite immunization with MUT30, tumor growth was slower and resulted in a 6 day increase in median survival (Figure 4B right). These data demonstrate that vaccination against a single mutation is able to confer antitumoral effects.

Discussion

Our study was motivated by the hypothesis that mutations provide a rich source for novel vaccine targets. While immunogenic mutations have been reported in mouse and man, there is a complete lack of knowledge regarding the fraction of non-synonymous mutations processed and presented in an immunological relevant manner. To address this question, we performed the first mouse tumor exome-capture study, identifying B16F10 somatic point mutations, followed by testing of mutations for their capability to elicit T-cell immunogenicity. Our result is the first map of the B16F10 "T-cell druggable mutanome".

The B16 melanoma cell line originated spontaneously in a C57BL/6 mouse in 1954 and was propagated by the Jackson Memorial Laboratory in Bar Harbor. *In vivo* passage of B16 cells resulted in formation of the highly metastatic daughter clone B16F10 (34). B16 cells express melanoma differentiation antigens and present MHC class I restricted epitopes from gp100, MART1 (35), tyrosinase (36), TRP1 (37) and TRP2 (30). Use of the B16F10 melanoma model has gained momentum in conjunction with vaccine research (38-41) and is today one of the most widely used cell lines for scientific validation of T-cell based immunotherapies (over 1,700 citations) and general cancer studies (over 13,000 citations). Mutation analyses of B16 cells have focused on prominent candidate genes, showing that *Cdkn2a* (cyclin-dependent kinase inhibitor 2A, $p19^{Arf}$ and $p16^{Ink4a}$) is homozygously deleted and that neither activating mutations in *Braf* nor inactivating mutations in *Trp53* are prevalent (42), but no unbiased genome-wide studies have been performed. Thus, the frequent use of B16 as a preclinical model stands in sharp contrast to the lack of knowledge of the genetic alterations that underlie the malignant phenotype and contribute to the repertoire of potential targets for T-cell based therapies.

We performed a meticulous mutation search using a novel NGS protocol and biostatistical algorithm we developed to identify mutations with high confidence. The B16F10 and parental (germline) C57BL/6 exomes were sequenced in triplicate (biological replicates), resulting in over 100 million reads per sample (over 620 million in total). The lack of reads aligning to the Y chromosome revealed that the B16F10 cells were derived from a female mouse. We identified a considerably higher number of mutations in B16 melanoma compared to primary human solid tumors, for which 16 to 302 non-synonymous mutations have been reported (26, 43, 44). Methods to identify and validate somatic mutations from NGS data are still in development, with recent studies reporting true positive rates of 54% (45) and largely unknown false negative rates. To confirm authenticity of mutation hits and exclude sequencing artifacts, we selected 50 of the identified somatic point mutations and were able to validate all 50 without exception. A likely explanation for the high number of mutations is that B16F10 has accumulated mutations over the five decades since it was established.

Whole-exome sequencing in combination with transcriptome profiling enables the discovery of the expressed protein coding mutanome and provides an insight into the molecular nature of potential driver mutations in B16 melanoma. The KEGG (Kyoto Encyclopedia of Genes and Genomes) (46) melanoma pathway (hsa05218) identifies four melanoma oncogenes (*Braf*, *Nras*, *Cdk4*, and *Mitf*) and three melanoma tumor suppressors (*Pten*, *Cdkn2a*, and *Trp53*). We found all three tumor suppressors to be mutated in B16F10. In contrast, none of the four KEGG-identified melanoma oncogenes displayed a mutation. However, we discovered mutations in associated

proteins of the respective pathways: *Rassf7* (RAS pathway), *Ksr1* (RAS pathway), *Atm* (PI3K/AKT pathway), and *Pdgfra* (RAS-MAPK/ERK pathway). Moreover, although not mutated, we detected overexpression of *Mitf*, suggestive of a transcriptional dysregulation. Furthermore, we identified a somatic mutation of *Trrap*, a gene identified earlier this year as a potential novel human target for malignant melanoma (27). Additional potential driver or enabling mutations in B16F10 include those in DNA repair machinery (*Brac*, *Rad9b*, *Atm*) and those associated with melanoma and cancer (e.g. *Alk*, *Aim1*, *Flt1*, *Pml*, *Mta3*, and *Fat1*).

For systematic immunogenicity testing, we selected 50 confirmed non-synonymous mutations that were abundantly expressed in B16F10 melanoma. We used long synthetic peptides for vaccination to simulate natural antigen processing and to allow presentation of both MHC I and II restricted epitopes (47, 48). RNA transfected DC as APCs for ELISPOT assays were used as independent method to confirm that immune responses recognize endogenously processed epitopes, additionally validating that the respective antigen fragment encoded by the RNA is processed and naturally presented.

As expected, only a subset of the B16F10 mutations is immunogenic. No apparent correlation was observed between immunogenicity with potential oncological relevance of the protein, structural features of the respective gene, or subcellular localization of the encoded protein. Importantly, we revealed the immunogenicity of novel somatic mutations that are not known to promote a malignant phenotype, such as those in *Actn4* (MUT46) and *Kif18b* (MUT30). Thus, regardless of their function, immunity against these mutations, as long as they are stably expressed in a relevant malignant cell population, may mediate tumor control. Indeed, a point mutation in the human *Actn4* ortholog was recently described in a lung cancer patient. The mutation created a tumor-specific HLA-A2 epitope that was presented and recognized by a

mutation specific CTL population that persisted over years in the blood of the patient, potentially influencing the positive course of the disease (49).

Our study allows estimation of the entire space of immunogenic tumor mutations (the T-cell druggable mutanome) in B16F10. We found one third (16 of 50) of the mutated epitopes to be immunogenic. Nearly half of these epitopes induced a strong T-cell response that matches the intensity observed for the H-2Kb restricted $Trp2_{180\text{-}188}$ epitope, which is one of the most immunogenic B16 melanoma target antigens. Thus, this study adds validated immunodominant epitopes to the target antigen space of B16 melanoma that qualify as candidates for antitumor vaccines. B16F10 contains 563 expressed, non-synonymous somatic mutations at FDR $\leq$ 0.05, with 430 of those predicted to be presented on MHC. We estimate that the B16F10 tumor mutanome, relative to the C57BL/6 mouse, comprises more than 180 immunogenic mutations with approximately 80 of them being able to mount strong immune responses.

B16 cells are poorly immunogenic and vaccination with irradiated tumor cells does not protect mice from subsequent challenge with living B16 cells (50, 51), in part due the low expression of MHC class I and absence of MHC class II molecules (52). Nevertheless, in our vaccination studies, we see antitumor effects for two of the tested mutated epitopes. The strong immune responses are able to compensate for the nearly complete down-regulation of MHC molecules in B16F10 melanoma cells (53). This interpretation is supported by the fact that after immunizing a group of mice with the immunodominant Trp2 epitope we observed comparable antitumor activity (Figure 4A).

This study has implications for human cancer therapies. Mutations in human TAAs that elicit both CD8 and CD4 T-cell epitopes have been described (8, 53). Human cancers carry on average

100-120 non-synonymous mutations. Segal *et al.* predicted 40 to 60 HLA class I restricted epitopes per patient derived from tumor specific somatic mutations (54). Given our identification of 563 expressed protein mutations in B16F10, the *in silico* prediction of Segal *et al.* matches to our estimate of 180 T-cell druggable mutations in B16F10 melanoma that is supported by experimental *in vivo* data. Even considering patient- and tumor-variability, this estimate suggests a rich T-cell druggable mutanome, which can be tapped by combining deep sequencing with systematic immunogenicity analysis of mutations. As a consequence, the approach opens a new dimension for individualized immunotherapy and adds to tailored vaccine concepts that were previously suggested by us and others (55-58). Every patient's tumor bears a highly individual mutation "signature" and more than 95% of mutations are unique and patient specific (1). Thus, a vaccine concept based on the multiplicity of mutated epitopes would require profiling of each patient's tumor to determine the unique mutation signature. Dramatically reduced costs and time required for genome-wide discovery of cancer specific mutations opens the door for individualized immunotherapy of cancer patients. In particular in advanced disease with tumor genomes becoming more unstable individualized T-cell therapies may outdo other treatment options as accumulation of mutations allows to combine even more antigens thereby counteracting the selection of antigen loss variants during immunotherapy and tumor evolution.

Acknowledgements

We thank M. Holzmann, R. Roth, M. Wagner, C. Kneip, T. Bukur and V. Boisguérin for assistance.

References

(1) Stratton MR. Exploring the genomes of cancer cells: progress and promise. Science 2011;331:1553-8.

(2) Wartman LD, Larson DE, Xiang Z, Ding L, Chen K, Lin L, et al. Sequencing a mouse acute promyelocytic leukemia genome reveals genetic events relevant for disease progression. J Clin Invest 2011;121:1445-55.

(3) Sjoblom T, Jones S, Wood LD, Parsons DW, Lin J, Barber TD, et al. The consensus coding sequences of human breast and colorectal cancers. Science 2006;314:268-74.

(4) Pleasance ED, Cheetham RK, Stephens PJ, McBride DJ, Humphray SJ, Greenman CD, et al. A comprehensive catalogue of somatic mutations from a human cancer genome. Nature 2010;463:191-6.

(5) Ding L, Ellis MJ, Li S, Larson DE, Chen K, Wallis JW, et al. Genome remodelling in a basal-like breast cancer metastasis and xenograft. Nature 2010;464:999-1005.

(6) Dubey P, Hendrickson RC, Meredith SC, Siegel CT, Shabanowitz J, Skipper JC, et al. The immunodominant antigen of an ultraviolet-induced regressor tumor is generated by a somatic point mutation in the DEAD box helicase p68. J Exp Med 1997;185:695-705.

(7) Ikeda H, Ohta N, Furukawa K, Miyazaki H, Wang L, Kuribayashi K, et al. Mutated mitogen-activated protein kinase: a tumor rejection antigen of mouse sarcoma. Proc Natl Acad Sci U S A 1997;94:6375-9.

(8) Lennerz V, Fatho M, Gentilini C, Frye RA, Lifke A, Ferel D, et al. The response of autologous T cells to a human melanoma is dominated by mutated neoantigens. Proc Natl Acad Sci U S A 2005;102:16013-8.

(9) Gnirke A, Melnikov A, Maguire J, Rogov P, LeProust EM, Brockman W, et al. Solution hybrid selection with ultra-long oligonucleotides for massively parallel targeted sequencing. Nat Biotechnol 2009;27:182-9.

(10) Waterston RH, Lindblad-Toh K, Birney E, Rogers J, Abril JF, Agarwal P, et al. Initial sequencing and comparative analysis of the mouse genome. Nature 2002;420:520-62.

(11) Langmead B, Trapnell C, Pop M, Salzberg SL. Ultrafast and memory-efficient alignment of short DNA sequences to the human genome. Genome Biol 2009;10:R25.

(12) Mortazavi A, Williams BA, McCue K, Schaeffer L, Wold B. Mapping and quantifying mammalian transcriptomes by RNA-Seq. Nat Methods 2008;5:621-8.

(13) Li H, Durbin R. Fast and accurate short read alignment with Burrows-Wheeler transform. Bioinformatics 2009;25:1754-60.

(14) Lundegaard C, Lamberth K, Harndahl M, Buus S, Lund O, Nielsen M. NetMHC-3.0: accurate web accessible predictions of human, mouse and monkey MHC class I affinities for peptides of length 8-11. Nucleic Acids Res 2008;36:W509-W512.

(15) Kumar P, Henikoff S, Ng PC. Predicting the effects of coding non-synonymous variants on protein function using the SIFT algorithm. Nat Protoc 2009;4:1073-81.

(16) Adzhubei IA, Schmidt S, Peshkin L, Ramensky VE, Gerasimova A, Bork P, et al. A method and server for predicting damaging missense mutations. Nat Methods 2010;7:248-9.

(17) Kreiter S, Selmi A, Diken M, Koslowski M, Britten CM, Huber C, et al. Intranodal vaccination with naked antigen-encoding RNA elicits potent prophylactic and therapeutic antitumoral immunity. Cancer Res 2010;70:9031-40.

(18) Lutz MB, Kukutsch N, Ogilvie AL, Rossner S, Koch F, Romani N, et al. An advanced culture method for generating large quantities of highly pure dendritic cells from mouse bone marrow. J Immunol Methods 1999;223:77-92.

(19) Holtkamp S, Kreiter S, Selmi A, Simon P, Koslowski M, Huber C, et al. Modification of antigen-encoding RNA increases stability, translational efficacy, and T-cell stimulatory capacity of dendritic cells. Blood 2006;108:4009-17.

(20) Kreiter S, Konrad T, Sester M, Huber C, Tureci O, Sahin U. Simultaneous ex vivo quantification of antigen-specific CD4+ and CD8+ T cell responses using in vitro transcribed RNA. Cancer Immunol Immunother 2007;56:1577-87.

(21) Sathirapongsasuti JF, Lee H, Horst BA, Brunner G, Cochran AJ, Binder S, et al. Exome sequencing-based copy-number variation and loss of heterozygosity detection: ExomeCNV. Bioinformatics 2011;27:2648-54.

(22) Pfeifer GP, You YH, Besaratinia A. Mutations induced by ultraviolet light. Mutat Res 2005;571:19-31.

(23) Zilfou JT, Lowe SW. Tumor suppressive functions of p53. Cold Spring Harb Perspect Biol 2009;1:a001883.

(24) Dey N, Crosswell HE, De P, Parsons R, Peng Q, Su JD, et al. The protein phosphatase activity of PTEN regulates SRC family kinases and controls glioma migration. Cancer Res 2008;68:1862-71.

(25) Verhaak RG, Hoadley KA, Purdom E, Wang V, Qi Y, Wilkerson MD, et al. Integrated genomic analysis identifies clinically relevant subtypes of glioblastoma characterized by abnormalities in PDGFRA, IDH1, EGFR, and NF1. Cancer Cell 2010;17:98-110.

(26) Hajra KM, Liu JR. Apoptosome dysfunction in human cancer. Apoptosis 2004;9:691-704.

(27) Wei X, Walia V, Lin JC, Teer JK, Prickett TD, Gartner J, et al. Exome sequencing identifies GRIN2A as frequently mutated in melanoma. Nat Genet 2011;43:442-6.

(28) Melief CJ, van der Burg SH. Immunotherapy of established (pre)malignant disease by synthetic long peptide vaccines. Nat Rev Cancer 2008;8:351-60.

(29) Datta SK, Redecke V, Prilliman KR, Takabayashi K, Corr M, Tallant T, et al. A subset of Toll-like receptor ligands induces cross-presentation by bone marrow-derived dendritic cells. J Immunol 2003;170:4102-10.

(30) Bloom MB, Perry-Lalley D, Robbins PF, Li Y, el-Gamil M, Rosenberg SA, et al. Identification of tyrosinase-related protein 2 as a tumor rejection antigen for the B16 melanoma. J Exp Med 1997;185:453-9.

(31) Schreurs MW, Eggert AA, de Boer AJ, Vissers JL, van HT, Offringa R, et al. Dendritic cells break tolerance and induce protective immunity against a melanocyte differentiation antigen in an autologous melanoma model. Cancer Res 2000;60:6995-7001.

(32) Echchakir H, Mami-Chouaib F, Vergnon I, Baurain JF, Karanikas V, Chouaib S, et al. A point mutation in the alpha-actinin-4 gene generates an antigenic peptide recognized by autologous cytolytic T lymphocytes on a human lung carcinoma. Cancer Res 2001;61:4078-83.

(33) Lee YM, Kim E, Park M, Moon E, Ahn SM, Kim W, et al. Cell cycle-regulated expression and subcellular localization of a kinesin-8 member human KIF18B. Gene 2010;466:16-25.

(34) Fidler IJ. Selection of successive tumour lines for metastasis. Nat New Biol 1973;242:148-9.

(35) Zhai Y, Yang JC, Spiess P, Nishimura MI, Overwijk WW, Roberts B, et al. Cloning and characterization of the genes encoding the murine homologues of the human melanoma antigens MART1 and gp100. J Immunother 1997;20:15-25.

(36) Mullins DW, Bullock TN, Colella TA, Robila VV, Engelhard VH. Immune responses to the HLA-A*0201-restricted epitopes of tyrosinase and glycoprotein 100 enable control of melanoma outgrowth in HLA-A*0201-transgenic mice. J Immunol 2001;167:4853-60.

(37) Overwijk WW, Lee DS, Surman DR, Irvine KR, Touloukian CE, Chan CC, et al. Vaccination with a recombinant vaccinia virus encoding a "self" antigen induces autoimmune vitiligo and tumor cell destruction in mice: requirement for CD4(+) T lymphocytes. Proc Natl Acad Sci U S A 1999;96:2982-7.

(38) Schwartzentruber DJ, Lawson DH, Richards JM, Conry RM, Miller DM, Treisman J, et al. gp100 peptide vaccine and interleukin-2 in patients with advanced melanoma. N Engl J Med 2011;364:2119-27.

(39) Slingluff CL, Jr., Petroni GR, Yamshchikov GV, Barnd DL, Eastham S, Galavotti H, et al. Clinical and immunologic results of a randomized phase II trial of vaccination using four melanoma peptides either administered in granulocyte-macrophage colony-stimulating factor in adjuvant or pulsed on dendritic cells. J Clin Oncol 2003;21:4016-26.

(40) Baumgaertner P, Jandus C, Rivals JP, Derre L, Lovgren T, Baitsch L, et al. Vaccination-induced functional competence of circulating human tumor-specific CD8 T-cells. Int J Cancer 2011.

(41) Wang F, Bade E, Kuniyoshi C, Spears L, Jeffery G, Marty V, et al. Phase I trial of a MART-1 peptide vaccine with incomplete Freund's adjuvant for resected high-risk melanoma. Clin Cancer Res 1999;5:2756-65.

(42) Melnikova VO, Bolshakov SV, Walker C, Ananthaswamy HN. Genomic alterations in spontaneous and carcinogen-induced murine melanoma cell lines. Oncogene 2004;23:2347-56.

(43) Lee W, Jiang Z, Liu J, Haverty PM, Guan Y, Stinson J, et al. The mutation spectrum revealed by paired genome sequences from a lung cancer patient. Nature 2010;465:473-7.

(44) Shah SP, Morin RD, Khattra J, Prentice L, Pugh T, Burleigh A, et al. Mutational evolution in a lobular breast tumour profiled at single nucleotide resolution. Nature 2009;461:809-13.

(45) Yoshida K, Sanada M, Shiraishi Y, Nowak D, Nagata Y, Yamamoto R, et al. Frequent pathway mutations of splicing machinery in myelodysplasia. Nature 2011;478:64-9.

(46) Kanehisa M, Goto S, Furumichi M, Tanabe M, Hirakawa M. KEGG for representation and analysis of molecular networks involving diseases and drugs. Nucleic Acids Res 2010;38:D355-D360.

(47) Bijker MS, van den Eeden SJ, Franken KL, Melief CJ, Offringa R, van der Burg SH. CD8+ CTL priming by exact peptide epitopes in incomplete Freund's adjuvant induces a vanishing CTL response, whereas long peptides induce sustained CTL reactivity. J Immunol 2007;179:5033-40.

(48) Zwaveling S, Vierboom MP, Ferreira Mota SC, Hendriks JA, Ooms ME, Sutmuller RP, et al. Antitumor efficacy of wild-type p53-specific CD4(+) T-helper cells. Cancer Res 2002;62:6187-93.

(49) Echchakir H, Mami-Chouaib F, Vergnon I, Baurain JF, Karanikas V, Chouaib S, et al. A point mutation in the alpha-actinin-4 gene generates an antigenic peptide recognized by autologous cytolytic T lymphocytes on a human lung carcinoma. Cancer Res 2001;61:4078-83.

(50) Dranoff G, Jaffee E, Lazenby A, Golumbek P, Levitsky H, Brose K, et al. Vaccination with irradiated tumor cells engineered to secrete murine granulocyte-macrophage colony-

stimulating factor stimulates potent, specific, and long-lasting anti-tumor immunity. Proc Natl Acad Sci U S A 1993;90:3539-43.

(51) Overwijk WW, Restifo NP. B16 as a mouse model for human melanoma. Curr Protoc Immunol 2001;Chapter 20:Unit.

(52) Seliger B, Wollscheid U, Momburg F, Blankenstein T, Huber C. Characterization of the major histocompatibility complex class I deficiencies in B16 melanoma cells. Cancer Res 2001;61:1095-9.

(53) Chen L, McGowan P, Ashe S, Johnston J, Li Y, Hellstrom I, et al. Tumor immunogenicity determines the effect of B7 costimulation on T cell-mediated tumor immunity. J Exp Med 1994;179:523-32.

(54) Segal NH, Parsons DW, Peggs KS, Velculescu V, Kinzler KW, Vogelstein B, et al. Epitope landscape in breast and colorectal cancer. Cancer Res 2008;68:889-92.

(55) Sahin U, Tureci O, Chen YT, Seitz G, Villena-Heinsen C, Old LJ, et al. Expression of multiple cancer/testis (CT) antigens in breast cancer and melanoma: basis for polyvalent CT vaccine strategies. Int J Cancer 1998;78:387-9.

(56) Sturniolo T, Bono E, Ding J, Raddrizzani L, Tuereci O, Sahin U, et al. Generation of tissue-specific and promiscuous HLA ligand databases using DNA microarrays and virtual HLA class II matrices. Nat Biotechnol 1999;17:555-61.

(57) Rammensee HG, Weinschenk T, Gouttefangeas C, Stevanovic S. Towards patient-specific tumor antigen selection for vaccination. Immunol Rev 2002;188:164-76.

(58) Hannani D, Sistigu A, Kepp O, Galluzzi L, Kroemer G, Zitvogel L. Prerequisites for the antitumor vaccine-like effect of chemotherapy and radiotherapy. Cancer J 2011;17:351-8.

Tables

Table 1. Mutations selected for validation. From left: assigned ID, gene symbol, amino acid substitution and position, gene name, predicted subcellular localization and type (Ingenuity).

ID	Symbol	Change	Entrez Gene Name	Subcellular localization	Type
MUT1	*Fzd7*	p.G304A	frizzled family receptor 7	Plasma Membrane	G-protein coupled receptor
MUT2	*Xpot*	p.I830S	exportin, tRNA (nuclear export receptor for tRNAs)	Nucleus	other
MUT3	*Ranbp2*	p.Q2871H	RAN binding protein 2	Nucleus	enzyme
MUT4	*Dnajb12*	p.P54T	DnaJ (Hsp40) homolog, subfamily B, member 12	Cytoplasm	other
MUT5	*Eef2*	p.G795A	eukaryotic translation elongation factor 2	Cytoplasm	translation regulator
MUT6	*Ptrf*	p.D382G	polymerase I and transcript release factor	Nucleus	transcription regulator
MUT7	*Trp53*	p.N128D	tumor protein p53	Nucleus	transcription regulator
MUT8	*Ddx23*	p.V602A	DEAD (Asp-Glu-Ala-Asp) box polypeptide 23	Nucleus	enzyme
MUT9	*Golgb1*	p.E2855D	golgin B1	Cytoplasm	other
MUT10	*Pcdhga11*	p.G82R	protocadherin gamma subfamily A, 11	Plasma Membrane	other
MUT11	*Snx15*	p.E211G	sorting nexin 15	Cytoplasm	transporter
MUT12	*Gnas*	p.S112G	GNAS (guanine nucleotide binding protein, alpha stimulating) complex locus	Plasma Membrane	enzyme
MUT13	*Fndc3b*	p.C561W	fibronectin type III domain containing 3B	Cytoplasm	other
MUT14	*Sbno1*	p.P309T	strawberry notch homolog 1 (Drosophila)	unknown	enzyme
MUT15	*Pi4k2b*	p.R344Q	phosphatidylinositol 4-kinase type 2 beta	Cytoplasm	kinase
MUT16	*Thumpd3*	p.T243S	THUMP domain containing 3	unknown	other
MUT17	*Tnpo3*	p.G504A	transportin 3	Cytoplasm	other
MUT18	*Numa1*	p.Q447K	nuclear mitotic apparatus protein 1	Nucleus	other
MUT19	*Wwp2*	p.E742K	WW domain containing E3 ubiquitin protein ligase 2	Cytoplasm	enzyme
MUT20	*Tubb3*	p.G402A	tubulin, beta 3	Cytoplasm	other
MUT21	*Atp11a*	p.R522S	ATPase, class VI, type 11A	Plasma Membrane	transporter
MUT22	*Asf1b*	p.A141P	ASF1 anti-silencing function 1 homolog B (S. cerevisiae)	Nucleus	other
MUT23	*Wdr82*	p.I221L	WD repeat domain 82	Nucleus	other
MUT24	*Dag1*	p.P425A	dystroglycan 1 (dystrophin-associated glycoprotein 1)	Plasma Membrane	transmembrane receptor
MUT25	*Plod2*	p.F530V	procollagen-lysine, 2-oxoglutarate 5-dioxygenase 2	Cytoplasm	enzyme
MUT26	*Orc2*	p.F278V	origin recognition complex, subunit 2	Nucleus	other
MUT27	*Obsl1*	p.T1764M	obscurin-like 1	unknown	other
MUT28	*Ppp1r7*	p.L170P	protein phosphatase 1, regulatory (inhibitor) subunit 7	Nucleus	phosphatase
MUT29	*Mthfd1l*	p.F294V	methylenetetrahydrofolate dehydrogenase (NADP+ dependent) 1-like	Cytoplasm	enzyme
MUT30	*Kif18b*	p.K739N	kinesin family member 18B	unknown	other
MUT31	*Ascc2*	p.A59G	activating signal cointegrator 1 complex subunit 2	unknown	other
MUT32	*Itsn2*	p.S1551R	intersectin 2	Cytoplasm	other
MUT33	*Pbk*	p.V145D	PDZ binding kinase	Cytoplasm	kinase
MUT34	*Klhl22*	p.F179V	kelch-like 22 (Drosophila)	unknown	other
MUT35	*Ddb1*	p.L438I	damage-specific DNA binding protein 1, 127kDa	Nucleus	other
MUT36	*Tm9sf3*	p.Y382H	transmembrane 9 superfamily member 3	Cytoplasm	transporter
MUT37	*Dpf2*	p.F275V	D4, zinc and double PHD fingers family 2	Nucleus	other
MUT38	*Atrn*	p.S745N	attractin	Extracellular Space	other
MUT39	*Snx5*	p.R373Q	sorting nexin 5	Cytoplasm	transporter
MUT40	*Armc1*	p.S85I	armadillo repeat containing 1	Cytoplasm	other
MUT41	*Ash1l*	p.L632I	ash1 (absent, small, or homeotic)-like (Drosophila)	Nucleus	transcription regulator
MUT42	*S100a13 2510039O18*	p.S18C	S100 calcium binding protein A13	Cytoplasm	other
MUT43	*Rik*	p.E391K	KIAA2013	unknown	other
MUT44	*Cpsf3l*	p.D314N	cleavage and polyadenylation specific factor 3-like	Nucleus	other
MUT45	*Mkrn1*	p.N346Y	makorin ring finger protein 1	unknown	other
MUT46	*Actn4*	p.F835V	actinin, alpha 4	Cytoplasm	other
MUT47	*Rpl13a*	p.A24G	ribosomal protein L13a	Cytoplasm	other
MUT48	*Def8*	p.R255G	differentially expressed in FDCP 8 homolog (mouse)	unknown	other
MUT49	*Fat1*	p.I1940M	FAT tumor suppressor homolog 1 (Drosophila)	Plasma Membrane	other
MUT50	*Sema3b*	p.L663V	sema domain, immunoglobulin domain (Ig), short basic domain, secreted, (semaphorin) 3B	Extracellular Space	other

Table 2. Summary of T-cell reactivities determined consecutive to vaccination with mutation encoding peptide. Statistical analysis was done by student´s t-test and Mann-Whitney test (non-parametric test). Responses were considered significant, when either test gave a p-value < 0,05 and the mean spot numbers were >30 spots/5x10^5 effector cells. Reactivities were rated by mean spot numbers -: <30; +: >30; ++: >50; +++ >200 spots/well.

Mutation	Gene Symbol	Reactivity against mutation	Reactivity against WT	Mutation	Gene Symbol	Reactivity against mutation	Reactivity against WT
MUT01	*Fzd7*	-	-	MUT26	Orc2	-	-
MUT02	*Xpot*	-	-	MUT27	Obsl1	-	-
MUT03	*Ranbp2*	-	-	MUT28	Ppp1r7	+	+
MUT04	*Dnajb12*	-	-	MUT29	Mthfd1l	+	-
MUT05	*Eef2*	+++	+++	MUT30	Kif18b	+++	-
MUT06	*Ptrf*	-	-	MUT31	Ascc2	-	-
MUT07	*Trp53*	-	-	MUT32	Itsn2	-	-
MUT08	*Ddx23*	-	-	MUT33	Pbk	-	-
MUT09	*Golgb1*	-	-	MUT34	Klhl22	-	-
MUT10	*Pcdhga11*	-	-	MUT35	Ddb1	-	-
MUT11	*Snx15*	-	-	MUT36	Tm9sf3	+	-
MUT12	*Gnas*	+	-	MUT37	Dpf2	-	-
MUT13	*Fndc3b*	-	-	MUT38	Atrn	-	-
MUT14	*Sbno1*	-	-	MUT39	Snx5	-	-
MUT15	*Pi4k2b*	-	-	MUT40	Armc1	-	-
MUT16	*Thumpd3*	-	-	MUT41	Ash1l	-	-
MUT17	*Tnpo3*	+++	++	MUT42	S100a13	-	-
MUT18	*Numa1*	-	-	MUT43	Rik	-	-
MUT19	*Wwp2*	-	-	MUT44	Cpsf3l	+++	++
MUT20	*Tubb3*	+++	-	MUT45	Mkrn1	++	++
MUT21	*Atp11a*	-	-	MUT46	Actn4	++	+
MUT22	*Asf1b*	++	++	MUT47	Rpl13a	-	-
MUT23	*Wdr82*	-	-	MUT48	Def8	++	++
MUT24	*Dag1*	++	+	MUT49	Fat1	-	-
MUT25	*Plod2*	+++	++	MUT50	Sema3b	+++	++

Figure Legends

Figure 1. **Discovery and characterization of the "T-cell druggable mutanome". (A)** Experimental procedure **. (B)** The mutation selection process for validation and immunogenicity testing, including numbers for B16. **(C)** The T-cell druggable mutanome mapped to the B16F10 genome. Rings from outside to inside: chromosomes, gene density (green), gene expression (green (low) to red (high)), and somatic mutations (orange): present in all triplicates; with FDR < 0.05; in protein coding regions; causing non-synonymous changes; in expressed genes; and the validated set.

Figure 2. **Immune responses elicited *in vivo* by vaccination of mice with mutation-representing long synthetic peptides. (A,B)** IFN-γ ELISPOT analysis of T-cell effectors from mice vaccinated with mutation coding peptides. Columns represent means (±SEM) of 5 mice per group. Asterisks indicate statistically significant differences of reactivity against mutation and wild-type peptide (student´s t-test; value $p < 0.05$). **(A)** Splenocytes of vaccinated mice were restimulated with BMDCs transfected with the mutation coding peptide used for vaccination, the corresponding wild-type peptide and an irrelevant control peptide (VSV-NP). **(B)** For analysis of T-cell reactivity against endogenously processed mutations splenocytes of vaccinated mice were restimulated with BMDCs transfected with control RNA (eGFP) or a RNA coding for the indicted mutation.

Figure 3. Mutation 30 (gene Kif18B, protein Q6PFD6, mutation p.K739N). Sanger sequencing traces and sequence of mutation (top) and protein domains and mutation location (bottom).

Figure 4. Antitumoral effects of mutated peptide vaccines in mice with aggressively growing B16F10 tumors (A) C57BL/6 mice (n = 7) were inoculated with 7.5 x 10^4 B16F10 cells s.c. into the flank of the mice. On day 3 and 10 after tumor inoculation the mice were vaccinated with 100 µg MUT30, MUT44 or Trp2 peptide + 50 µg poly(I:C), with adjuvant alone, or left untreated. Accumulated data from two separate experiments. The data are presented as means ±SEM. **(B)** C57BL/6 mice (n = 5) received one immunization of 100 µg MUT30 peptide + 50 µg poly(I:C) on day -4. On day 0 7.5 x 10^4 B16F10 cells were inoculated s.c. into the flank of the mice. Booster immunizations with MUT30 peptid (+ poly(I:C)) were done on days 2 and 9. Control mice were left untreated. Kaplan-Meier survival Blot (left). Accumulated data from two separate experiments. Tumor growth kinetics (right), the data are presented as means ±SEM.

Author Manuscript Published OnlineFirst on January 11, 2012; DOI: 10.1158/0008-5472.CAN-11-3722

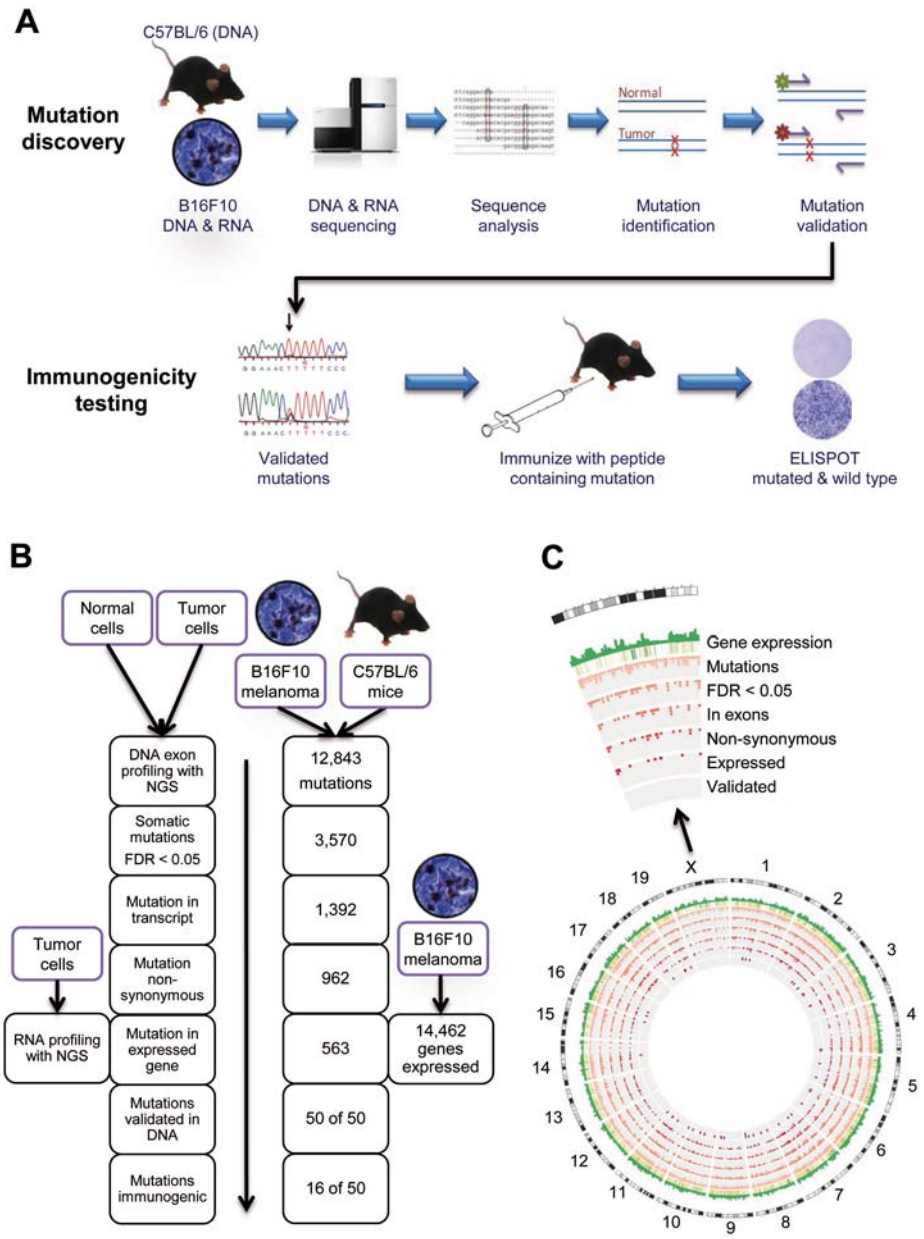

Author Manuscript Published OnlineFirst on January 11, 2012; DOI: 10.1158/0008-5472.CAN-11-3722
Author manuscripts have been peer reviewed and accepted for publication but have not yet been edited.

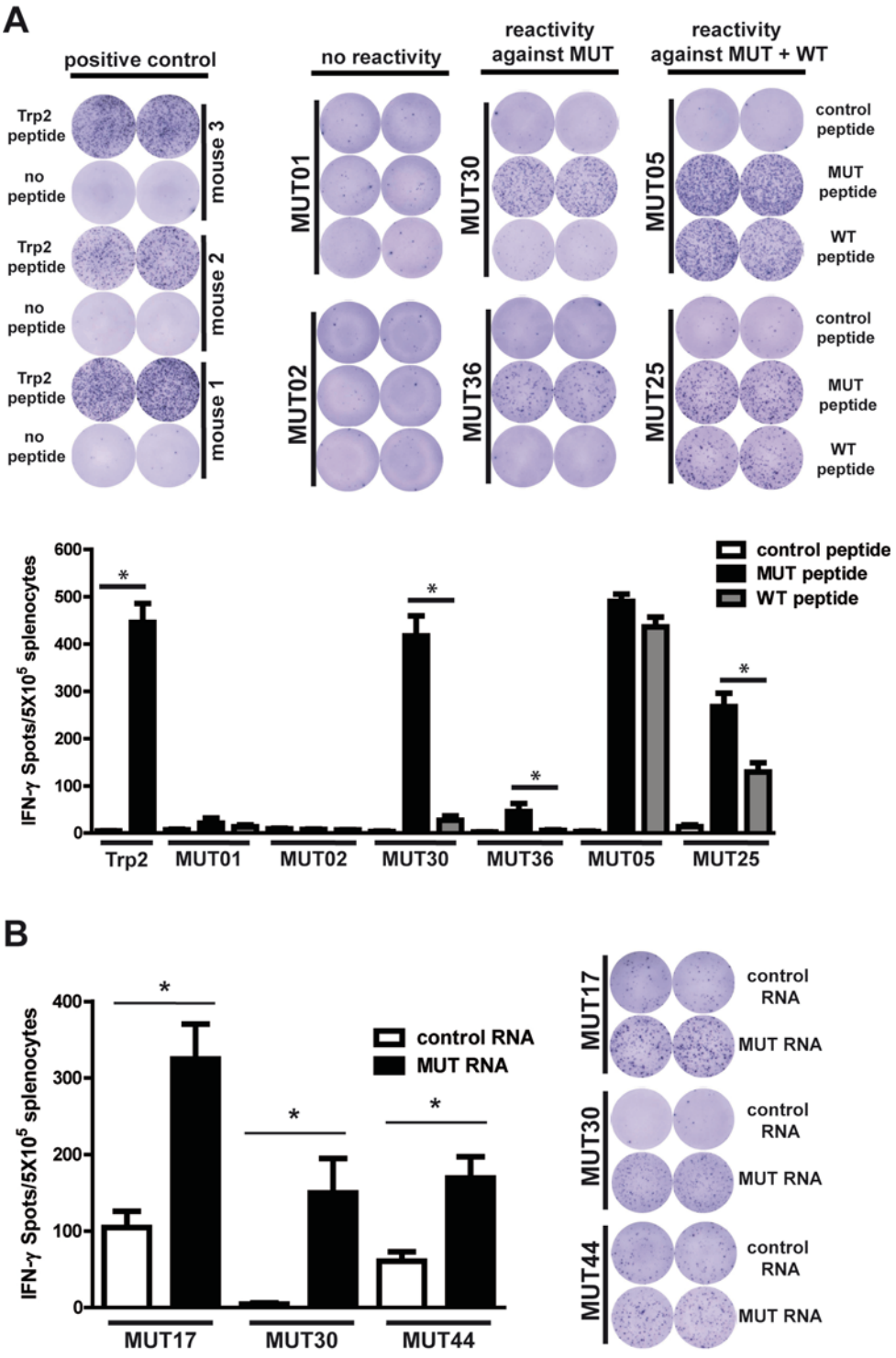

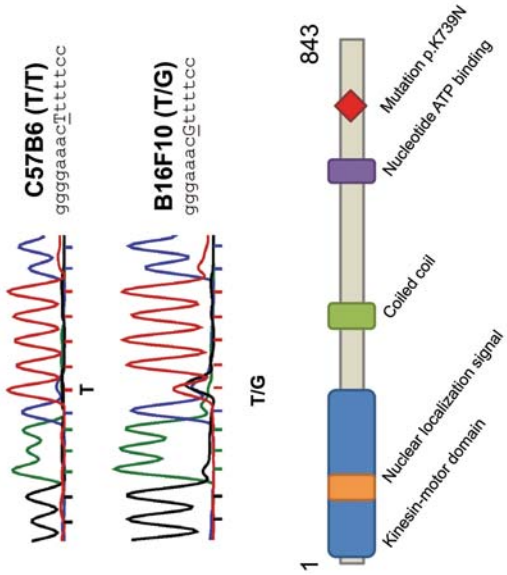

Author Manuscript Published OnlineFirst on January 11, 2012; DOI: 10.1158/0008-5472.CAN-11-3722
Author manuscripts have been peer reviewed and accepted for publication but have not yet been edited.

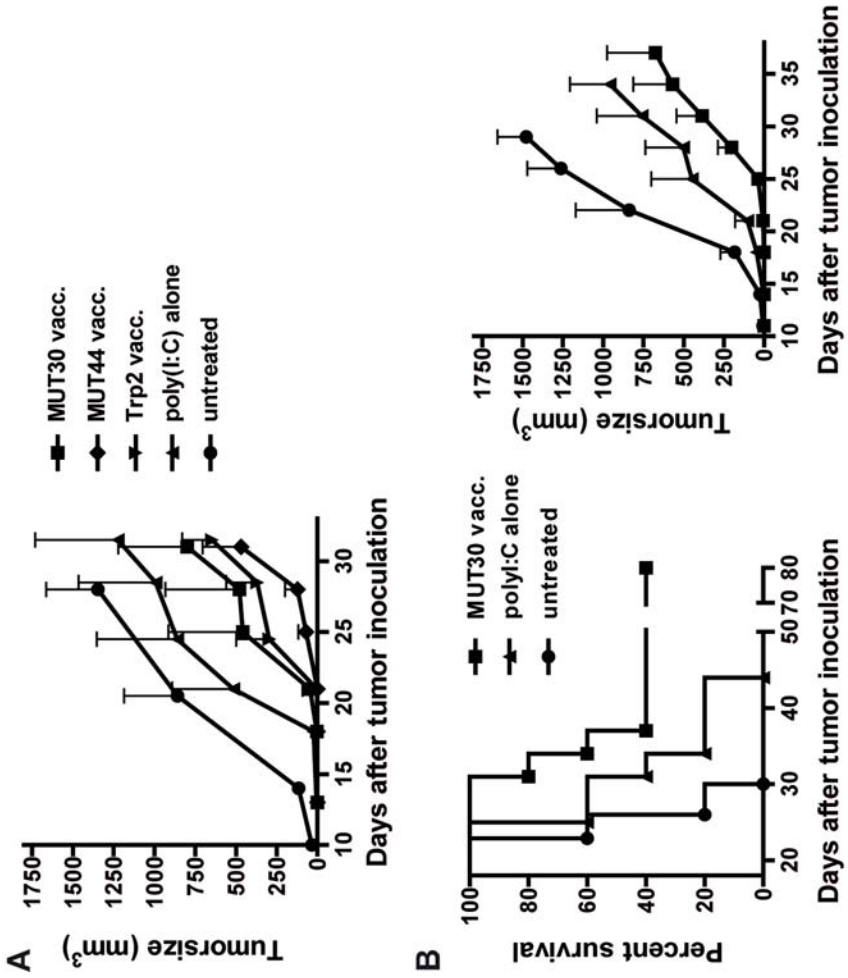

AACR American Association for Cancer Research

Cancer Research

The Journal of Cancer Research (1916–1930) | The American Journal of Cancer (1931–1940)

Exploiting the mutanome for tumor vaccination

John C. Castle, Sebastian Kreiter, Jan Diekmann, et al.

Cancer Res Published OnlineFirst January 11, 2012.